Dead Reckoning of a Biped Robot on Various Terrain by Kalman Filter Adaptive to Ground Reaction Force

Ken Masuya[1] and Tomomichi Sugihara[2]

Abstract— **A novel Kalman filter to estimate position of a biped robot is proposed. It combines the kinematics and the double-integral of acceleration, only using internal sensors and achieving high-rate estimation. The kinematics computation is rooted to the anchoring pivot, which is the most invariant point in the foot with respect to the ground. The idea is the same with the authors previous method, but the estimation accuracy has been largely improved by referring to the ground reaction force. Namely, the anchoring pivot is estimated based on both the velocity information and the force information. The efficacy of the proposed method is verified through simulations of walking and hopping motions.**

I. Introduction

A high-rate position control of legged robots requires an accurate position estimation at the same or higher rate. Present external sensors such as cameras[1], laser range finders[2] and a combination of them[3] are not available for this purpose due to their low sampling rate. On the other hand, internal sensors such as encoders and accelerometers can measure physical quantities faster than the above external sensors, so they possibly work with a technique to estimate by information only from internal sensors, namely, dead reckoning.

In the field of legged robots, the kinematics computation, which one can know the relative location of the robot body with respect to the supporting foot through and thus we call the foot-based kinematics, hereafter, is used[4], [5]. However, its accuracy is easily lowered when the supporting foot rolls or rotates. Furthermore, it does not work when the robot hops. Nishiwaki et al.[6] used the zero-moment point (ZMP[7]) to correct the posture error caused by unexpected rotation due to the topography, but its accuracy depends on the performance of the controller. Another option is to use an accelerometer[8], the double-integral of which provides the position information regardless to the foot contact condition, though it suffers from the error accumulation. In order to improve the accuracy of the estimation, some methods to use Kalman filter[9], [10], [11], [12], [13], [14] were proposed. Chilian et al.[9] and Bloesch et al.[10] assumed that the foot contacts to the ground at the point or the foot was a small hemisphere shape, so that they cannot be applied to robots with a large foot, which are supposed to work in a standing posture. Xinjilefu et al.[11] designed an extended Kalman filter (EKF) based on the five-link model. Oriolo et al.[12] proposed EKF combining the foot-based kinematics and visual information. Those assume that the supporting foot contacts stationarily to the ground during the stance. Ahn et al.[13] proposed a Kalman filter for dynamic motions including the heel and toe contact phase. However, the foot-based kinematics in this paper is also disturbed by the ground contact at the part of the sole. The supporting foot can move in various way with respect to the ground, and in general situations, it is difficult to know how they move during a step in advance. Rotella et al.[14] dealt with the movement of supporting foot as the noise. However, in dynamic motions, the magnitude of the noise varies with the motion.

This paper proposes a Kalman filter which takes the movement of the supporting foot into consideration. In contrast to our previous work[15], this paper focuses on the time property of the noise of the kinematics computation, but it is difficulty to model the noise due to the effect by the motion and the contact condition of the supporting foot. For the difficulty, the proposed filter employs the anchoring pivot (AP), which corresponds to the minimum velocity point in the author's previous work[15], as the pivot of the foot-based kinematics. Thus, AP can make modeling the noise easier, while the estimation accuracy of AP is improved. The previous version had a shortcoming that it was sensitive to the error of attitude estimation. This is mitigated by fusing ZMP on each sole.

II. Kalman filter reflected the foot contact condition for AP-based dead reckoning

Our goal is to estimate $\boldsymbol{p}_0$ and $\boldsymbol{v}_0$ which are the position and velocity of the body frame Σ_0 with respect to the inertial frame Σ, respectively. For this purpose, the filter, which combines $\boldsymbol{p}_0$ obtained by the foot-based kinematics computation with that obtained by the double integral of acceleration (DIA), is designed based on the frequency or time domain. The design based on the former one needs the complementarity of signals, but it has the advantage of easier tuning of parameters if the frequency properties of signals or noises are empirically known. On the other hand, that on the latter has the difficulty in tuning of parameters, but it can deal with the certainty of signals. Namely, the main difference between them is how to deal with the property of noises. Now, we consider the properties of signals for dead reckoning, DIA is high-reliable in the high frequency domain, namely, it depends on the frequency domain. On the other hand, noises included in the kinematics computation depend

*This work was supported by Grant-in-Aid for Challenging Exploratory Research #26540135, Japan Society for the Promotion of Science

[1]K. Masuya is with the Department of Adaptive Machine Systems, Graduate School of Engineering, Osaka University, Japan ken.masuya@ams.eng.osaka-u.ac.jp

[2]T. Sugihara is with the Department of Adaptive Machine Systems, Graduate School of Engineering, Osaka University, Japan zhidao@ieee.org

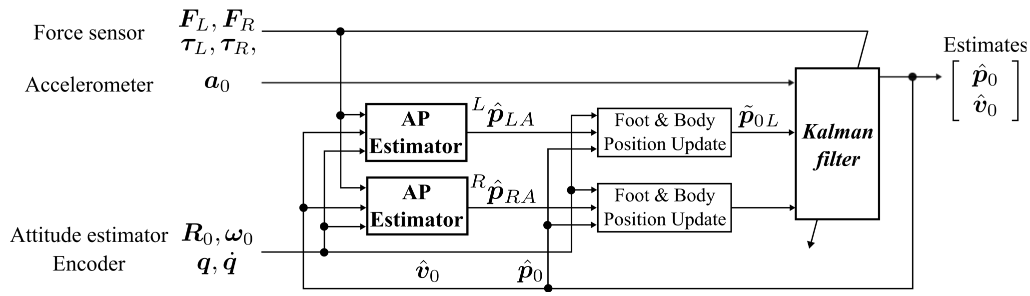

Fig. 1. The proposed Kalman filter

on the time domain rather than the frequency one. Thus, our previous work[15] designed a complementary filter based on the frequency property of DIA. In contrast, this paper designs a Kalman filter by focusing on the time-dependency of the noise property of the kinematics computation. However, the difficulty of tuning still remains. It is due to that the noise is affected by the motion and the contact of the supporting foot which are accompanied with the locomotion.

In order to simplify the noise model, this paper lowers the effect of the motion of the supporting foot by using AP-rooted kinematics computation, thus the noise is approximated as the function only of the contact condition and white noise. Regarding the kinematics computation from each foot as the observation model, the model is written as

$$\boldsymbol{y} = \begin{bmatrix} \mathbf{1} & \boldsymbol{O} \\ \mathbf{1} & \boldsymbol{O} \end{bmatrix} \boldsymbol{x} + \begin{bmatrix} \mathbf{1} \\ \mathbf{1} \end{bmatrix} \boldsymbol{e}_p + \boldsymbol{E}(\boldsymbol{f}_L, \boldsymbol{f}_R)\boldsymbol{w}_o, \tag{1}$$

where $\boldsymbol{x} = \left[\boldsymbol{p}_0^{\mathrm{T}}\ \boldsymbol{v}_0^{\mathrm{T}}\right]^{\mathrm{T}}$. $\mathbf{1}, \boldsymbol{O} \in \mathbb{R}^{3\times 3}$ are the identity matrix and the zero matrix, respectively. $\boldsymbol{E}(\boldsymbol{f}_L, \boldsymbol{f}_R) \in \mathbb{R}^{6\times 6}$ is the coefficient matrix of the observation noise $\boldsymbol{w}_o \in \mathbb{R}^6$ to reflect the variation of reliability in accordance with the ground reaction force acting on the left foot $\boldsymbol{f}_L$ and the right foot $\boldsymbol{f}_R$ under the assumption that the magnitude of the force is related to the foot contact condition. Tuning of those are detailed in Section IV. $\boldsymbol{y} = \left[\tilde{\boldsymbol{p}}_{0L}^{\mathrm{T}}\ \tilde{\boldsymbol{p}}_{0R}^{\mathrm{T}}\right]^{\mathrm{T}}$. $\tilde{\boldsymbol{p}}_{0L}$ and $\tilde{\boldsymbol{p}}_{0R}$ mean $\boldsymbol{p}_0$ obtained from the left foot frame Σ_L and the right foot frame Σ_R by AP-rooted kinematics computation, respectively. AP computation is detailed in Section III. The measurement is computed based on the estimate one step before, so that the position error of the estimate one step before $\boldsymbol{e}_p \in \mathbb{R}^3$ is included in the observation model. In the kinematics computation, $\boldsymbol{R}_0$ and $\boldsymbol{\omega}_0$, which mean the attitude and angular velocity of Σ_0 with respect to Σ, respectively, are supposed to be given by the attitude estimator[16], in advance. The joint angles and those derivatives, which are used to obtain the relative values between the body and each foot, are measured by encoders accurately.

On the other hand, the acceleration is regarded as the input, a process model is written as

$$\dot{\boldsymbol{x}} = \begin{bmatrix} \boldsymbol{O} & \mathbf{1} \\ \boldsymbol{O} & \boldsymbol{O} \end{bmatrix} \boldsymbol{x} + \begin{bmatrix} \boldsymbol{O} \\ \mathbf{1} \end{bmatrix} (\boldsymbol{a}_0 - \boldsymbol{g}) + \boldsymbol{w}_s, \tag{2}$$

where $\boldsymbol{g} = [0\ 0\ g]^{\mathrm{T}}$, $g = 9.8[\mathrm{m/s}^2]$ is the acceleration due to the gravity. $\boldsymbol{a}_0$ is the acceleration of Σ_0 with respect to Σ and is measured by an accelerometer. $\boldsymbol{w}_s \in \mathbb{R}^6$ denotes the process noise which tuning of is also detailed in Section IV.

The proposed Kalman filter is designed for the system constructed by Eqs. (1) and (2). Its observability and controllability are easily confirmed. Fig. 1 shows the overview of the proposed method which sequence is composed of the following steps:

i) AP estimation on each foot based on the velocity and force constraint.
ii) Updating the position of each foot and the body.
iii) Kalman filter designed for the system represented by Eqs. (1) and (2).

III. AP COMPUTATION BASED ON THE VELOCITY AND THE FORCE CONSTRAINT

The following discussion can be applied to both feet, so that this section only focuses on Σ_L. In previous work[15], the position of AP on Σ_L, $\boldsymbol{p}_{LA}$, was obtained as

$$\boldsymbol{p}_{LA} = \boldsymbol{p}_L + \boldsymbol{R}_L\, {}^L\boldsymbol{p}_{LA}, \tag{3}$$

where $\boldsymbol{p}_L$ and $\boldsymbol{R}_L$ are the position and attitude of Σ_L with respect to Σ, respectively, and computed as

$$\boldsymbol{p}_L = \boldsymbol{p}_0 + \boldsymbol{R}_0\, {}^0\boldsymbol{p}_L, \tag{4}$$

$$\boldsymbol{R}_L = \boldsymbol{R}_0\, {}^0\boldsymbol{R}_L. \tag{5}$$

${}^0\boldsymbol{p}_L$ and ${}^0\boldsymbol{R}_L$ represent the relative position and attitude between Σ_0 and Σ_L, respectively, and are obtained by encoders and the link parameters. If ${}^L\boldsymbol{p}_{LA}$ can be computed, then $\boldsymbol{p}_0$ and $\boldsymbol{p}_L$ can be updated based on Eqs. (3) and (4).

In order to estimate ${}^L\boldsymbol{p}_{LA}$, we focused on the differential kinematics on the foot. The estimate ${}^L\hat{\boldsymbol{p}}_{LA}$ was computed as the minimizer of the following evaluation function:

$$E = E_1 + \frac{1}{T_m^2} E_2, \tag{6}$$

where T_m is the positive time constant working as the weight. E_1 and E_2 mean the evaluation functions expressing the global velocity of AP and the regularization term, respectively, and are written as

$$E_1 = \frac{1}{2} \|\boldsymbol{v}_L + \boldsymbol{\omega}_L \times \boldsymbol{R}_L\, {}^L\hat{\boldsymbol{p}}_{LA}\|^2, \tag{7}$$

$$E_2 = \frac{1}{2} \|\delta\, {}^L\hat{\boldsymbol{p}}_{LA}\|^2. \tag{8}$$

${}^L\hat{\boldsymbol{p}}_{LA}$ is an instantaneous variable, so that ${}^L\hat{\boldsymbol{v}}_{LA}$ equals the zero vector $\mathbf{0} \in \mathbb{R}^3$. Thus, $\delta\, {}^L\hat{\boldsymbol{p}}_{LA}$ is not ${}^L\hat{\boldsymbol{p}}_{LA}$ but the variation between ${}^L\hat{\boldsymbol{p}}_{LA}$ at a certain moment and at the next moment. $\boldsymbol{v}_L$ and $\boldsymbol{\omega}_L$ are the velocity and angular velocity of Σ_L with respect to Σ, respectively, and calculated as

$$\boldsymbol{v}_L = \boldsymbol{v}_0 + \boldsymbol{\omega}_0 \times \boldsymbol{R}_0 \, {}^0\boldsymbol{p}_L + \boldsymbol{R}_0 \, {}^0\boldsymbol{v}_L, \tag{9}$$

$$\boldsymbol{\omega}_L = \boldsymbol{\omega}_0 + \boldsymbol{R}_0 \, {}^0\boldsymbol{\omega}_L. \tag{10}$$

${}^0\boldsymbol{v}_L$ and ${}^0\boldsymbol{\omega}_L$ denote the relative velocity and angular velocity between Σ_0 and Σ_L, respectively, and can be computed as well as ${}^0\boldsymbol{p}_L$ and ${}^0\boldsymbol{R}_L$. Eq. (9) uses the tentative estimate of $\boldsymbol{v}_0$. However, $\boldsymbol{v}_L$ obtained by Eq. (9) becomes inaccurate due to the attitude error, even if $\boldsymbol{v}_0$ is the ground truth. Namely, ${}^L\hat{\boldsymbol{p}}_{LA}$ based on Eq. (6) is sensitive to that error.

In order to reduce the influence of the attitude error, this paper computes ${}^L\hat{\boldsymbol{p}}_{LA}$ by using the evaluation function representing the line of force action through ZMP of each sole addition to the above functions. This idea is based on the assumption that the largest force acts on the point with the least motion and the point with that force exists on that line. The equation of the moment on that line is written as

$$ {}^L\boldsymbol{\tau}_L + \left({}^L\boldsymbol{p}_{LF} - {}^L\hat{\boldsymbol{p}}_{LA}\right) \times {}^L\boldsymbol{f}_L = \boldsymbol{0}, \tag{11}$$

where ${}^L\boldsymbol{\tau}_L$ and ${}^L\boldsymbol{f}_L$ are the torque and the force which are represented on Σ_L and measured by the force sensor attached on the left foot, respectively. ${}^L\boldsymbol{p}_{LF}$ is the position of the force sensor on Σ_L. Therefore, ${}^L\hat{\boldsymbol{p}}_{LA}$ is computed as the minimizer of the following evaluation function:

$$E = \alpha_1 E_1 + \frac{1}{\zeta_2} E_2 + \alpha_3 \frac{1}{\zeta_3} E_3, \tag{12}$$

$$E_3 = \frac{1}{2} \| {}^L\boldsymbol{\tau}_L + \left({}^L\boldsymbol{p}_{L,F} - {}^L\hat{\boldsymbol{p}}_{LA}\right) \times {}^L\boldsymbol{f}_L \|^2, \tag{13}$$

where α_1 and α_3 are the positive weights for E_1 and E_3, respectively. The weight for E_2 is necessary to regularize, so that it is set to 1.0. ζ_2 and ζ_3 are the positive constant to convert the dimension into the square of the velocity. After the computation of ${}^L\hat{\boldsymbol{p}}_{LA}$, the estimates $\tilde{\boldsymbol{p}}_L$ and $\tilde{\boldsymbol{p}}_{0L}$ are obtained by kinematics.

Likewise, ${}^R\hat{\boldsymbol{p}}_{RA}$, $\tilde{\boldsymbol{p}}_R$ and $\tilde{\boldsymbol{p}}_{0R}$ can be computed.

IV. Implementation of the Proposed Method

A. Proposed Kalman filter

A discretization is required to implement the proposed method on the computer. Hereafter, ΔT denotes the sampling interval and $*_k$ means the value of the variable $*$ at $k\Delta T$.

First, Eqs. (1) and (2) are represented in discretized way by the forward difference approximation, as

$$\boldsymbol{x}_{k+1} = \boldsymbol{A}\boldsymbol{x}_k + \boldsymbol{B}\left(\boldsymbol{a}_k - \boldsymbol{g}\right) + \Delta T \boldsymbol{w}_{s,k}, \tag{14}$$

$$\boldsymbol{y}_k = \boldsymbol{C}\boldsymbol{x}_k + \boldsymbol{D}\boldsymbol{e}_{p,k} + \boldsymbol{E}(\boldsymbol{f}_{L,k}, \boldsymbol{f}_{R,k})\boldsymbol{w}_{o,k}, \tag{15}$$

where

$$\boldsymbol{A} = \begin{bmatrix} \boldsymbol{1} & \Delta T \boldsymbol{1} \\ \boldsymbol{O} & \boldsymbol{1} \end{bmatrix}, \boldsymbol{B} = \begin{bmatrix} \boldsymbol{O} \\ \Delta T \boldsymbol{1} \end{bmatrix}, \boldsymbol{C} = \begin{bmatrix} \boldsymbol{1} & \boldsymbol{O} \\ \boldsymbol{1} & \boldsymbol{O} \end{bmatrix}, \boldsymbol{D} = \begin{bmatrix} \boldsymbol{1} \\ \boldsymbol{1} \end{bmatrix}.$$

Suppose that $\boldsymbol{E}(\boldsymbol{f}_{L,k}, \boldsymbol{f}_{R,k})$ is a diagonal matrix, its components correspond to the reliability of each foot-based kinematics. For this reason, its value should be large when the foot is unlikely to contact on the ground, namely, when

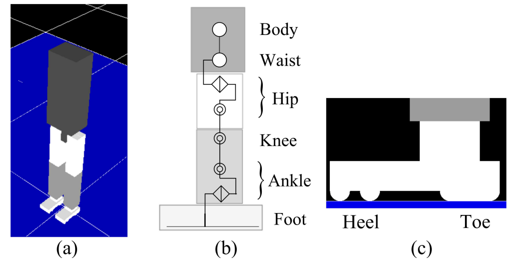

Fig. 2. The robot model. (a)The exterior. (b)The structure. (c)The shape of the foot

the force is small. On the other hand, the larger value the force sensor outputs, the smaller value the component is. Therefore, this paper designs $\boldsymbol{E}(\boldsymbol{f}_{L,k}, \boldsymbol{f}_{R,k})$ as

$$\boldsymbol{E}(\boldsymbol{f}_{L,k}, \boldsymbol{f}_{R,k}) = \begin{bmatrix} \frac{1}{\eta \hat{f}_{Lz,k}+1}\boldsymbol{1} & \boldsymbol{O} \\ \boldsymbol{O} & \frac{1}{\eta \hat{f}_{Rz,k}+1}\boldsymbol{1} \end{bmatrix}, \tag{16}$$

where η is the positive constant. $\hat{f}_{*z,k}$ is the non-dimensional value arranged the upper bound and the lower bound of the vertical component of $\boldsymbol{f}_{*,k}$ by using the robot mass M, as

$$\hat{f}_{*z,k} = \begin{cases} 0 & (f_{*z,k} < 0) \\ \frac{f_{*z,k}}{Mg} & (0 \le f_{*z,k} < Mg) \\ 1 & (Mg \le f_{*z,k}) \end{cases} \quad (* = L \, \text{or} \, R), \tag{17}$$

Let $\hat{\boldsymbol{x}}_k$ and $\bar{\boldsymbol{x}}_k$ be the estimated and the predictive value of $\boldsymbol{x}_k$, respectively, Kalman filter for the system represented by Eqs. (14) and (15) is composed of the following steps:

$$\boldsymbol{K}_k = \bar{\boldsymbol{P}}_{x,k}\boldsymbol{C}^{\mathrm{T}}\left(\boldsymbol{C}\bar{\boldsymbol{P}}_{x,k}\boldsymbol{C}^{T} + \boldsymbol{S}_{o,k}\right)^{-1}, \tag{18}$$

$$\boldsymbol{S}_{o,k} = \boldsymbol{D}\hat{\boldsymbol{P}}_{p,k-1}\boldsymbol{D}^{\mathrm{T}} + \boldsymbol{E}_k\boldsymbol{P}_o\boldsymbol{E}_k^{\mathrm{T}}, \tag{19}$$

$$\hat{\boldsymbol{x}}_k = \bar{\boldsymbol{x}}_k + \boldsymbol{K}_k\left(\boldsymbol{y}_k - \boldsymbol{C}\bar{\boldsymbol{x}}_k\right), \tag{20}$$

$$\hat{\boldsymbol{P}}_{x,k} = \bar{\boldsymbol{P}}_{x,k} - \boldsymbol{K}_k\boldsymbol{C}\bar{\boldsymbol{P}}_{x,k}, \tag{21}$$

$$\bar{\boldsymbol{x}}_{k+1} = \boldsymbol{A}\hat{\boldsymbol{x}}_k + \boldsymbol{B}\left(\boldsymbol{a}_k - \boldsymbol{g}\right), \tag{22}$$

$$\bar{\boldsymbol{P}}_{x,k+1} = \boldsymbol{A}\hat{\boldsymbol{P}}_{x,k}\boldsymbol{A}^{\mathrm{T}} + \boldsymbol{P}_s. \tag{23}$$

where $\boldsymbol{P}_s$, $\boldsymbol{P}_o \in \mathbb{R}^{6\times 6}$ are the covariance matrices of $\boldsymbol{w}_s\Delta T$ and $\boldsymbol{w}_o$, respectively. Hereafter, $\boldsymbol{P}_s$ and $\boldsymbol{P}_o$ are assumed as the diagonal matrix which components are represented by $\sigma_{s,ii}$ and $\sigma_{o,ii}$, respectively. $\hat{\boldsymbol{P}}_{x,k}$ and $\bar{\boldsymbol{P}}_{x,k}$ are the error covariance matrices of $\hat{\boldsymbol{x}}_k$ and $\bar{\boldsymbol{x}}_k$, respectively. $\hat{\boldsymbol{P}}_{p,k} \in \mathbb{R}^{3\times 3}$ mean the covariance matrix of $\boldsymbol{e}_p$ which corresponds the matrix of the upper left of $\hat{\boldsymbol{P}}_{x,k}$.

Finally, the tuning of $\sigma_{s,ii}$, $\sigma_{o,ii}$ and ϵ is described. Since $\sigma_{s,ii}$ $(i = 4,5,6)$ is mainly due to the acceleration noise, it is designed based on Allan variance[17] of the accelerometer. For easy tuning, this paper uses the average of them σ_{sv}. On the other hand, $\sigma_{s,ii}$ $(i = 1,2,3)$ is due to the discrete noise rather than the above noise, so that it is represented by a parameter σ_{sp}. $\sigma_{o,ii}$ and ϵ represents the reliability of the kinematics computation when the foot is on the ground and in the air, thus the variances in those situations, which are denoted by $\sigma_{o\,\min}$ and $\sigma_{o\,\max}$, respectively, are determined at first. They represents a reliability of kinematics computation relative to that of DIA, so that they are determined as

$$\sigma_{o\,\min} = 0.1\sigma_{sp}, \quad \sigma_{o\,\max} = 1000\sigma_{sp}. \tag{24}$$

Then, $\sigma_{o,ii}$ and ϵ are computed as

$$\sigma_{o,ii} = \sigma_{o\max}, \quad \eta = \sqrt{\frac{\sigma_{o\max}}{\sigma_{o\min}}} - 1. \tag{25}$$

B. AP estimation

For the implementation, it is also required to represent Eq. (12) in discretized way and to show its computability. E_1 , E_2 and E_3 shown in Section III are discretized as

$$E_1 = \frac{1}{2}\|\bar{\boldsymbol{v}}_{L,k} + \boldsymbol{\omega}_{L,k} \times \boldsymbol{R}_{L,k}\,{}^{L}\hat{\boldsymbol{p}}_{LA,k}\|^2, \tag{26}$$

$$E_2 = \frac{1}{2}\|\,{}^{L}\hat{\boldsymbol{p}}_{LA,k} - {}^{L}\hat{\boldsymbol{p}}_{LA,k-1}\|^2, \tag{27}$$

$$E_3 = \frac{1}{2}\|{}^{L}\boldsymbol{\tau}_{L,k} + \left({}^{L}\boldsymbol{p}_{LF} - {}^{L}\hat{\boldsymbol{p}}_{LA,k}\right) \times {}^{L}\boldsymbol{f}_{L,k}\|^2. \tag{28}$$

where $\bar{\boldsymbol{v}}_L$ is obtained by putting the predicted value $\bar{\boldsymbol{v}}_0$ into Eq. (9). This paper set ζ_2 and ζ_3 as $\zeta_2 = \Delta T^2$ and $\zeta_3 = (Mg\Delta T)^2$, respectively. The following equation is obtained by the stationary condition $\left(\frac{\partial E}{\partial\,{}^{L}\hat{\boldsymbol{p}}_{LA,k}}\right)^{\mathrm{T}} = \boldsymbol{0}$:

$$\boldsymbol{G}_{L,k}\,{}^{L}\hat{\boldsymbol{p}}_{LA,k} = \boldsymbol{u}_{L,k}, \tag{29}$$

where

$$\begin{aligned}
\boldsymbol{G}_{L,k} &= \frac{1}{\zeta_2}\boldsymbol{1} - \alpha_1\left[{}^{L}\boldsymbol{\omega}_k\times\right]^2 - \frac{\alpha_3}{\zeta_3}\left[{}^{L}\boldsymbol{f}_{L,k}\times\right]^2, \\
\boldsymbol{u}_{L,k} &= \frac{1}{\zeta_2}{}^{L}\hat{\boldsymbol{p}}_{LA,k-1} + \alpha_1\left[{}^{L}\boldsymbol{\omega}_k\times\right]\boldsymbol{R}_{L,k}^{\mathrm{T}}\bar{\boldsymbol{v}}_{L,k} \\
&\quad + \frac{\alpha_3}{\zeta_3}\left[{}^{L}\boldsymbol{f}_{L,k}\times\right]\left({}^{L}\boldsymbol{\tau}_{L,k} - \left[{}^{L}\boldsymbol{f}_{L,k}\times\right]{}^{L}\boldsymbol{p}_{LF}\right)
\end{aligned}$$

and ${}^{L}\hat{\boldsymbol{\omega}}_k = \boldsymbol{R}_{L,k}^{\mathrm{T}}\boldsymbol{\omega}_{L,k}$. Since $\boldsymbol{G}_{L,k}$ is the positive matrix, it is easily confirmed that ${}^{L}\hat{\boldsymbol{p}}_{LA,k}$ can be computed by Eq. (29). By using ${}^{L}\hat{\boldsymbol{p}}_{LA,k}$, $\tilde{\boldsymbol{p}}_{L,k}$ and $\tilde{\boldsymbol{p}}_{0L,k}$ are computed as

$$\begin{aligned}
\tilde{\boldsymbol{p}}_{L,k} &= \hat{\boldsymbol{p}}_{0,k-1} + \boldsymbol{R}_{0,k-1}\,{}^{0}\boldsymbol{p}_{L,k-1} \\
&\quad - \boldsymbol{R}_{L,k}\,{}^{L}\hat{\boldsymbol{p}}_{LA,k} + \boldsymbol{R}_{L,k-1}\,{}^{L}\hat{\boldsymbol{p}}_{LA,k}, \qquad (30) \\
\tilde{\boldsymbol{p}}_{0L,k} &= \tilde{\boldsymbol{p}}_{L,k} - \boldsymbol{R}_{0,k}\,{}^{0}\boldsymbol{p}_{L,k}. \qquad (31)
\end{aligned}$$

Likewise, ${}^{R}\hat{\boldsymbol{p}}_{RA,k}$, $\tilde{\boldsymbol{p}}_{R,k}$ and $\tilde{\boldsymbol{p}}_{0R,k}$ can be computed.

V. Evaluation by Simulation

A. Set up

Simulations were executed on the dynamics simulator OpenHRP3[18] with a robot shown in Fig. 2. An accelerometer and force sensors are attached on the body and each ankle of the robot, respectively. In simulations, we set to $M = 10.0$[kg] and $\Delta T = 2$[ms]. The reference of joint angles and those differential, which are given to PD controller, were computed based on Yamamoto et al.[19] in advance. Both the static and kinetic coefficient were set to 1.0.

In this paper, the following methods are compared:

- The foot-based kinematics without AP (FK)
- DIA with a high-pass filter (DIA+HPF)
- The complementary filter proposed in [15] (Previous)
- The proposed method (Proposed)

Table I shows parameters of Proposed which were tuned by about 100 trials and errors for one datum. $\sigma_{o,ii}$ and ϵ are determined based on Eqs. (24) and (25). Parameters of Previous were the same as that in [15] except for T_m. In order to evaluate the effect of E_3, the weight for E_2 in Eqs. (6) and (12) were arranged, namely, $T_m = \Delta T$. A high-pass filter used in DIA+HPF was also the same as that in [15].

TABLE I
PARAMETERS OF THE PROPOSED METHOD

Parameter	σ_{sp}	σ_{sv}	α_1	α_3
Value	0.001	0.0085	1.0	0.01

TABLE II
THE ERROR OF ESTIMATION FOR WALKING

	Method	x	y	z	3D
Position [mm]	FK	40.09	35.98	43.29	69.10
	DIA+HPF	123.3	105.7	52.69	170.7
	Previous	38.25	30.26	47.34	67.97
	Proposed	35.59	32.70	13.09	50.07
Velocity [mm/s]	FK	1029.4	1009.8	167.2	1451.6
	DIA+HPF	142.1	136.9	72.75	210.3
	Previous	150.8	152.4	74.68	227.1
	Proposed	85.75	84.59	34.79	125.4

TABLE III
THE ERROR OF ESTIMATION FOR JUMPING

	Method	x	y	z	3D
Position [mm]	FK	36.59	47.27	331.1	336.4
	DIA+HPF	342.5	366.3	199.1	539.5
	Previous	115.1	121.6	88.81	189.5
	Proposed	102.1	108.5	43.00	155.0
Velocity [mm/s]	FK	859.7	1122.1	1670.6	2188.4
	DIA+HPF	240.0	262.4	181.1	399.0
	Previous	198.9	200.3	153.6	321.3
	Proposed	147.9	150.6	134.4	250.2

Let $\mathcal{N}(\boldsymbol{\mu}, \boldsymbol{\Sigma})$ be the normal distribution represented by the mean $\boldsymbol{\mu}$ and the covariance matrix $\boldsymbol{\Sigma}$, the following errors are considered in order to imitate sensor noises:

$$\boldsymbol{e}_a \sim \mathcal{N}(\boldsymbol{\mu}_a, 0.1^2\boldsymbol{1}_3), \quad \boldsymbol{\mu}_a \sim \mathcal{N}(\boldsymbol{0}, 0.04^2\boldsymbol{1}_3), \tag{32}$$

$$\boldsymbol{e}_f \sim \mathcal{N}(\boldsymbol{0}, 1.0^2\boldsymbol{1}_3), \quad \boldsymbol{e}_\tau \sim \mathcal{N}(\boldsymbol{0}, 0.01^2\boldsymbol{1}_3), \tag{33}$$

$$\boldsymbol{e}_R = \frac{3.0}{(1 + (1/10\pi)s)^2}\boldsymbol{w}_R, \quad \boldsymbol{w}_R \sim \mathcal{N}(0, 0.1^2\boldsymbol{1}_3), \tag{34}$$

where $\boldsymbol{e}_a$, $\boldsymbol{e}_f$, $\boldsymbol{e}_\tau$ and $\boldsymbol{e}_R$ mean the error of acceleration, force, torque and attitude, respectively. $\boldsymbol{w}_R$ was filtered by 2nd-order low-pass filter to imitate both the attitude error and the angular velocity error. $\boldsymbol{e}_a$, $\boldsymbol{e}_f$ and $\boldsymbol{e}_\tau$ were simply added to true values and $\boldsymbol{e}_R$ was added to Euler angles corresponding to $\boldsymbol{R}_0$. The mean $\boldsymbol{\mu}_a$ was initialized at the beginning of each simulation. The simulation was run 1000 times in all for one motion.

B. Walking on the plane

As shown in Fig. 3, the robot walks forward with the heel and toe contact. First, it is evaluated that AP-rooted kinematics computation reduces the effect on the noise by the motion of the foot. The relationship between the absolute value of position errors of the kinematics computation from the left foot and $\hat{f}_{Lz,k}$ without attitude error is plotted in Fig. 4. The result shows that the motion affects noises from the kinematics computation without AP. On the other hand, AP-rooted kinematics computation can reduce the effect.

The root-mean-square error (RMSE) of the position and velocity estimation is shown in Table II. Figs. 5 and 6 show

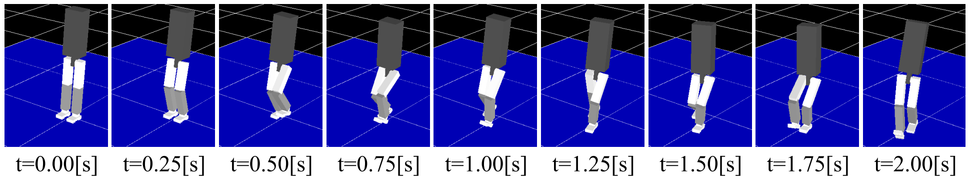

Fig. 3. The snapshots of walking on the plane

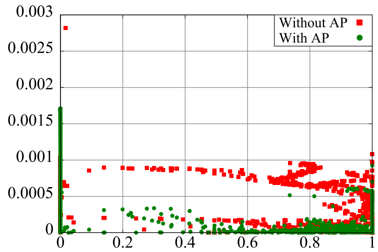

(a) x-direction

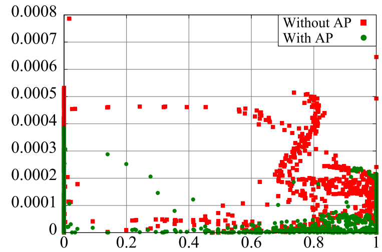

(b) y-direction

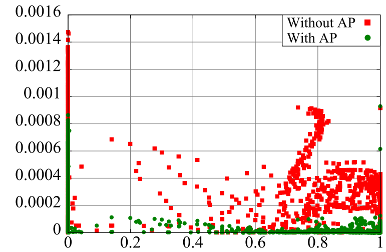

(c) z-direction

Fig. 4. The relationship between the absolute value of position errors of the kinematics computation from the left foot(vertical : [m]) and $\hat{f}_{Lz}$(horizontal).

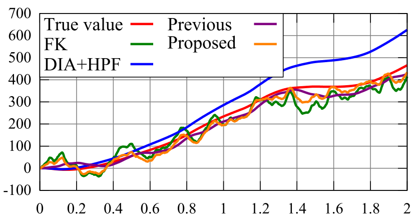

(a) x-direction

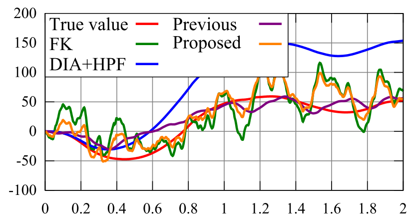

(b) y-direction

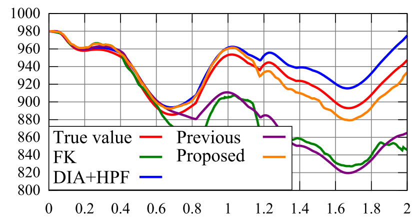

(c) z-direction

Fig. 5. A result of position estimation for walking on the plane. (The vertical axis is position[mm] and the horizontal one is time[s].)

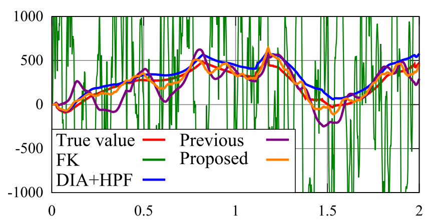

(a) x-direction

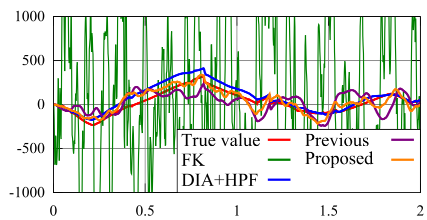

(b) y-direction

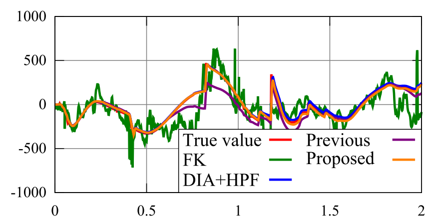

(c) z-direction

Fig. 6. A result of position estimation for walking on the plane. (The vertical axis is velocity[mm/s] and the horizontal one is time[s].)

an example of the result. From the result, FK can roughly follow the ground truth in x and y direction. However, its accuracy in z direction is lowered due to the change in height caused by the rolling of the supporting foot. Although DIA+HPF can estimate the velocity more accurate than the above method, its accuracy of position estimation suffers from the error accumulation. Previous is accurate moderately, but it is strongly affected by the foot-based kinematics because T_m is designed as the small value. Proposed can be more accurate in both estimations than other methods. Especially, compared with Previous, 3D-RMSE can reduced about 25[%] in the position estimations and 30[%] in the velocity estimation. This is mainly due to the existence of E_3, so that the efficacy of the novel AP computation is verified.

C. Jumping

As shown in Fig. 7, the robot squats down first and jumps forward diagonally afterwards. Table III shows RMSE of the position and velocity estimation. An example of the result is plotted in Figs. 8 and 9.

As expected, FK cannot follow the true motion of z direction during the jumping. DIA+HPF follows that motion comparatively, but its accuracy is degraded by the error accumulation as well as the case of walking. Compared with them, both Previous and Proposed are improved by taking the reliability varied with the foot contact condition into consideration. Additionally, RMSE of Proposed is about 25 [%] less in both estimations than Previous due to the improvement of AP computation.

VI. Conclusion

For the dead reckoning of biped robots, this paper proposes a novel Kalman filter which combines the foot-based kinematics and the acceleration basically. The accuracy of the foot-based kinematics is improved by using AP as the pivot of the kinematics. The sensitivity to the attitude error, which the previous computation of AP has, is lowered by considering the force constraint. Additionally, the observa-

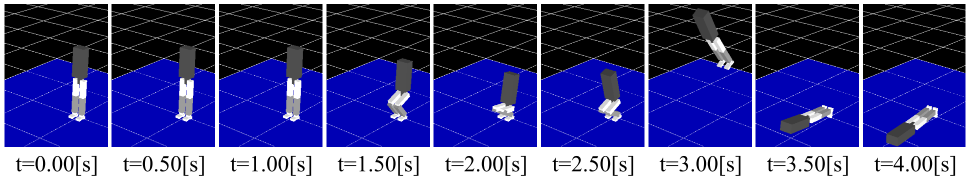

Fig. 7. The snapshots of jumping

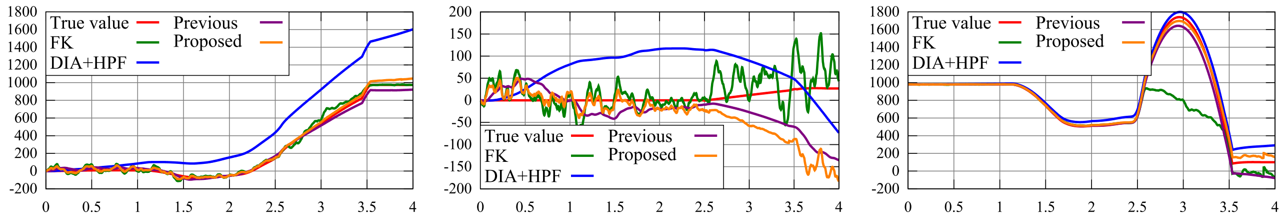

(a) x-direction (b) y-direction (c) z-direction

Fig. 8. A result of position estimation for jumping. (The vertical axis is position[mm] and the horizontal one is time[s].)

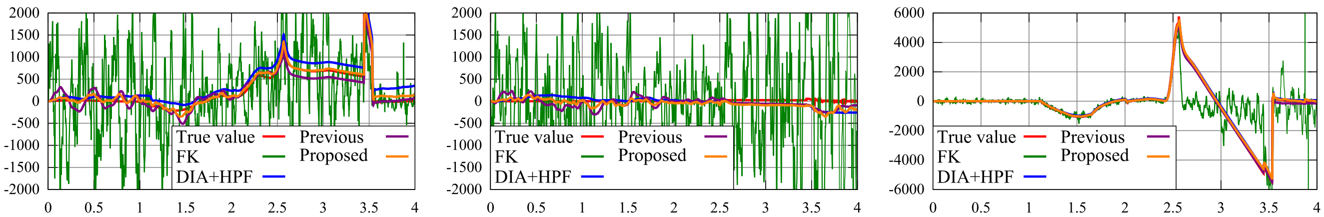

(a) x-direction (b) y-direction (c) z-direction

Fig. 9. A result of velocity estimation for jumping. (The vertical axis is velocity[mm/s] and the horizontal one is time[s].)

tion error is adaptively varied with the ground reaction force in order to reflect the variation of the relative reliability. The simulation result shows that the proposed method can reduce RMSE compared with the our previous method.

References

[1] S. Thompson and S. Kagami, "Humanoid Robot Localisation using Stereo Vision," Proc. of the 2005 IEEE-RAS Int. Conf. on Humanoid Robots, pp.19-25, 2005.

[2] A Hornung, K. M. Wurm and M. Bennewitz, "Humanoid Robot Localization in Complex Indoor Environments," Proc of the 2010 IEEE/RSJ Int. Conf. on Intelligent Robots and Systems, pp.1690-1695, 2010.

[3] S. Oßwald, A. Hornung and M. Bennewitz, "Improved Proposals for Highly Accurate Localization Using Range and Vision Data," Proc. of the 2012 IEEE/RSJ Int. Conf. on Intelligent Robots and Systems, pp.1809-1814, 2012.

[4] G. P. Roston and E. P. Krotkov, "Dead Reckoning Navigation for Walking Robots," Proc. of the 1992 IEEE/RSJ Int. Conf. on Intelligent Robots and Systems, pp.607-612, 1992.

[5] T. Masuda, Y. Mae, T. Arai, K. Inoue, "Dead Reckoning of Multi-legged Robot," Human Friendly Mechatronics, selected papers of the International Conference on Machine Automation, pp.351-356, 2000.

[6] K. Nishiwaki, J. Chestnutt and S. Kagami, "Autonomous navigation of a humanoid robot over unknown rough terrain using a laser range sensor," The Int. J. of Robotics Research, vol.31, no.11, pp.1251-1262, 2012.

[7] M. Vukobratović and J. Stepanenko, "On The Stability of Anthropomorphic Systems," Mathematical Biosciences, vol.15, No.1, pp.1-37, 1972.

[8] L. Marques, J. Lobo, J. Dias, U. Nunes and A. T. de Almeida, "Sensors for Legged Mobile Robots," Proc. of 2nd Int. Workshop on Climbing & Walking Robots, pp.33-58, 1999.

[9] A. Chilian, H. Hirschmüller, M. Görner, "Multisensor Data Fusion for Robust Pose Estimation of a Six-Legged Walking Robot," Proc. of the 2011 IEEE/RSJ Int. Conf. on Intelligent Robots and Systems, pp.2497-2504, 2011.

[10] M. Bloesch, M. Hutter, M. Hoepflinger, S. Leutenegger, C. Gehring, C. D. Remy and R. Siegwart, "State Estimation for Legged Robots - Consistent Fusion of Leg Kinematics and IMU," Proc. of Robotics: Science and Systems, 2012.

[11] Xinjilefu and C. G. Atkeson, "State Estimation of a Walking Humanoid Robot," Proc. of the 2012 IEEE/RSJ Int. Conf. on Intelligent Robots and Systems, pp.3693-3699, 2012.

[12] G. Oriolo, A. Paolillo, L. Rosa and M. Vendittelli, "Vision-Based Odometric Localization for Humanoids using a Kinematic EKF," Proc. of the 12th IEEE-RAS Int. Conf. on Humanoid Robots, pp.153-158, 2012.

[13] S. H. Ahn, S. Yoon, S. Hyung, N. Kwak and K. S. Roh, "On-board Odometry Estimation for 3D Vision-based SLAM of Humanoid Robot," Proc. of the 2012 IEEE/RSJ Int. Conf. on Intelligent Robots and Systems, pp.4006-4012, 2012.

[14] N. Rotella, M. Bloesch, L. Righetti and S. Schaal, "State Estimation for a Humanoid Robot," Proc. of the 2014 IEEE/RSJ Int. Conf. on Intelligent Robots and Systems, pp.952-958, 2014.

[15] K. Masuya and T. Sugihara, "A Dual-Stage Complementary Filter for Dead Reckoning of a Biped Robot Via Estimated Contact Point," Proc. of the 2013 IEEE-RAS Int. Conf. on Humanoid Robots, pp.112-117, 2013.

[16] K. Masuya, T. Sugihara and M. Yamamoto, "Design of Complementary Filter for High-fidelity Attitude Estimation based on Sensor Dynamics Compensation with Decoupled Properties," Proc. of the 2012 IEEE Int. Conf. on Robotics and Automation, pp.606-611, 2012.

[17] D.W. Allan, "Time and Frequency (Time-Domain) Characterization, Estimation, and Prediction of Precision Clocks and Oscillators," IEEE Trans. on Ultrasonics, Ferroelectrics and Frequency Control, vol.34, no.6, pp.647-654, 1987.

[18] S. Nakaoka, S. Hattori, F. Kanehiro, S. Kajita and H. Hirukawa, "Constraint-based Dynamics Simulator for Humanoid Robots with Shock Absorbing Mechanisms," Proc. of The 2007 IEEE/RSJ Int. Conf. on Intelligent Robots and Systems, pp.3641-3647, 2007

[19] K. Yamamoto, T. Sugihara and Y. Nakamura, "Gait Planning including Toe Contact with Boundary Condition Relaxation," Proc. of the 17th CISM-IFToMM Symposium, pp.409-416, 2008.